

perature to 77°K. Figures 3 and 4 provide quantitative experimental verification of Eq. (2)<sup>7</sup> and consequently verification of the dispersion relation (1).

*Note added in proof.* Jones and Chambers<sup>6</sup> have measured  $R$  for Li, Na, K, In, and Al using the resonance

method in thin slabs. For sodium they find  $R = -24.6 \times 10^{-11} \text{ m}^3/\text{C} \pm 1\%$  at 4°K.

We are grateful to S. Tallman for contributions to the experiment and to R. H. Silsbee for helpful discussions.

## Nuclear Polarization in Polycrystalline Holmium-Indium Alloy\*

V. L. SAILOR, R. I. SCHERMER, F. J. SHORE,† C. A. REYNOLDS,‡ H. MARSHAK, AND HANS POSTMA§

Brookhaven National Laboratory, Upton, New York

(Received March 29, 1962)

Holmium and indium nuclei have been polarized by nuclear hyperfine interaction in a polycrystalline ferromagnetic alloy, 92.2% holmium–7.8% indium. The nuclear polarization for each constituent was determined from the transmission of monochromatic, polarized neutron beams at neutron energies corresponding to resonances in the holmium and indium cross sections. A series of measurements at several temperatures from 0.071 to 4.225°K yield the following values for the hyperfine constant: for holmium,  $A/k = 0.58 \pm 0.03^\circ\text{K}$  (corresponding to an effective field at the nucleus,  $H_{\text{eff}} = +8.4 \times 10^6 \text{ Oe}$ ); and for In,  $A/k = -0.013 \pm 0.002^\circ\text{K}$  (corresponding to  $H_{\text{eff}} = -1.3 \times 10^6 \text{ Oe}$ ). The effect on the nuclear polarization of the magnetic anisotropy of the polycrystalline sample is discussed.

### I. INTRODUCTION

RECENT measurements<sup>1</sup> have demonstrated that large nuclear polarization ( $\sim 0.4$ ) occurs in holmium metal at relatively high temperatures (0.95°K). The polarization originates from an unusually large nuclear hyperfine interaction, which also occurs in various holmium compounds, e.g., holmium ethyl sulphate.<sup>2</sup> The existence of this large hyperfine interaction was independently confirmed by the specific heat measurements on holmium metal by Gordon, Dempsey, and Soller<sup>3</sup> who obtained the value  $A/k = 0.618^\circ\text{K}$  for the nuclear hyperfine interaction constant. Since our initial publication,<sup>1</sup> we have extended our measurements to both higher and lower temperatures. These new data yield a more precise value of  $A/k$  as well as providing additional facts about the magnetic nature of holmium metal at low temperatures.

The sample which was used for the new measurements was actually an alloy of 92.2% holmium–7.8% indium (at. %).<sup>4</sup> As will be seen, this alloy is ferromagnetic at low temperatures and, for the holmium atoms, appears

to retain the value of  $A/k$  which is characteristic of pure holmium metal. There are several reasons for studying an Ho–In alloy: (1) The sign and magnitude of the hyperfine interaction at the diamagnetic indium in the strongly ferromagnetic rare-earth lattice are of interest, *per se*. (2) We are interested in finding suitable ferromagnetic “host” materials in which various impurity nuclei can be polarized, and which differ from iron with respect to alloying properties. (3) Another more technical reason of interest was to verify the fact that the sample comes to thermal equilibrium with the refrigerating salt at the lowest temperatures obtained during the reported measurements.

It appears that the “host” method is potentially useful for producing reasonably large nuclear polarization in many elements which normally can be polarized only by the “brute force” method. Existing data<sup>5–7</sup> indicate that the effective magnetic field at an impurity nucleus in a ferromagnetic host material can have a magnitude as large as  $10^5$  to  $10^6 \text{ Oe}$ . Since the fields which are practical and presently available for use in the brute

\* Work performed under the auspices of the U. S. Atomic Energy Commission.

† Permanent address: Queens College, Flushing, New York.

‡ Permanent address: University of Connecticut, Storrs, Connecticut.

§ Permanent address: Kamerlingh Onnes Laboratorium, Leiden, the Netherlands.

<sup>1</sup> H. Postma, H. Marshak, V. L. Sailor, F. J. Shore, and C. A. Reynolds, *Phys. Rev.* **126**, 979 (1962).

<sup>2</sup> J. M. Baker, and B. Bleaney, *Proc. Phys. Soc. (London)* **A68**, 1090 (1955).

<sup>3</sup> J. E. Gordon, C. W. Dempsey, and T. Soller, *Phys. Rev.* **124**, 724 (1961).

<sup>4</sup> This alloy was kindly prepared by C. F. Klamut of the Metallurgy Division of Brookhaven National Laboratory.

<sup>5</sup> B. N. Samoilov, V. V. Sklyarevskii, and E. P. Stepanov, *J. Exptl. Theoret. Phys. (U.S.S.R.)* **36**, 644 (1959) [translation: *Soviet Phys.—JETP* **9**, 448 (1959)]; *J. Exptl. Theoret. Phys. (U.S.S.R.)* **36**, 1944 (1959) [translation: *Soviet Phys.—JETP* **9**, 1383 (1959)]; *J. Exptl. Theoret. Phys. (U.S.S.R.)* **38**, 359 (1960) [translation: *Soviet Phys.—JETP* **11**, 261 (1960)]; and B. N. Samoilov, V. V. Sklyarevskii, V. D. Gorobchenko, and E. P. Stepanov, *J. Exptl. Theoret. Phys. (U.S.S.R.)* **40**, 1871 (1961) [translation: *Soviet Phys.—JETP* **13**, 1314 (1961)].

<sup>6</sup> A. V. Kogan, V. D. Kul'kov, L. P. Nikitin, N. M. Reinov, I. A. Sokolov and M. F. Stel'makh, *J. Exptl. Theoret. Phys. (U.S.S.R.)* **39**, 47 (1960) [translation: *Soviet Phys.—JETP* **12**, 34 (1961)]; and *J. Exptl. Theoret. Phys. (U.S.S.R.)* **40**, 109 (1961) [translation: *Soviet Phys.—JETP* **13**, 78 (1961)].

<sup>7</sup> L. D. Roberts and J. O. Thomson, *Bull. Am. Phys. Soc.* **6**, 75, 230 (1961).

force method are of the order of 20 000 Oe (or possibly  $10^5$  Oe with superconducting solenoids), the "host" method offers enormous advantages when it can be used.

## II. EFFECTIVE NUCLEAR POLARIZATION IN HOLMIUM METAL

### A. Magnetic Structure

Holmium metal is ferromagnetic at temperatures below  $\sim 20^\circ\text{K}$  and the magnetic structure is strongly anisotropic<sup>8-10</sup> with respect to the crystalline axes. This anisotropy, which persists even in the presence of applied fields in excess of 70 000 Oe,<sup>11</sup> results in different saturation magnetization  $M_s$  for polycrystalline and single-crystal specimens. The ratio  $M_s(\text{poly})/M_s(\text{single})$  can be calculated for various simple models; however, no single model is expected to be adequate for all ranges of applied fields because of changes in the magnetic structure which are theoretically predicted at various critical fields.<sup>12</sup>

The neutron diffraction data of Koehler *et al.*<sup>13</sup> provide a plausible model for the magnetic structure for the case of a moderate external field ( $H_0 \approx 10$  to 30 kOe) applied at some arbitrary angle to the  $c$  axis. It appears that the magnetic moment lies entirely in the basal plane and in one of six "easy" directions within this plane. Note that only a small component of field perpendicular to the  $c$  axis destroys the small  $c$  component which exists under zero-field conditions. We shall assume that when the metal is magnetized to saturation the moment in each crystallite lies along that easy direction which gives the maximum component along  $H_0$ . If the crystallites in a polycrystalline sample are randomly oriented we then obtain for the polycrystal/single-crystal ratio of saturation magnetization

$$\frac{M_s(\text{poly})}{M_s(\text{single})} = \frac{\int_0^{\pi/2} \cos^2 \theta d\theta \int_0^{\pi/6} \cos \beta d\beta}{\int_0^{\pi/2} \cos \theta d\theta \int_0^{\pi/6} d\beta} = 0.75. \quad (1)$$

If the sample is not magnetized to saturation, we assume that in some domains the moment does not lie along the particular easy direction which gives the maximum component along  $H_0$ , but lies along one of the other easy directions. Thus, in this model, the magnetization of unsaturated polycrystalline metal to

saturated single crystal is

$$K_m(H_0) = \frac{M_H(\text{poly})}{M_s(\text{poly})} \frac{M_s(\text{poly})}{M_s(\text{single})}. \quad (2)$$

An experimental curve at  $1.3^\circ\text{K}$  for the first ratio was published by Henry<sup>11</sup> for one specimen of holmium metal. Although we expect individual specimens to show wide variations in the magnetization curves, we can obtain a rough estimate from his curve for our magnetizing field of 17 kOe,

$$M_H(\text{poly})/M_s(\text{poly}) \approx 0.8,$$

in which we have included a small correction ( $\sim 2\%$ ) for the demagnetization due to the slab geometry of our sample. Thus, we estimate  $K_m(H_0=17 \text{ kOe}) \approx 0.8 \times 0.75 \approx 0.6$ . As will be seen in Sec. VA, our data yield the experimental value  $K_m=0.48$ .

### B. Nuclear Polarization in Polycrystalline Holmium

The effective nuclear polarization will be less in a polycrystalline metal than in a single crystal because of the strong anisotropy discussed above. In each domain the axis of quantization will coincide with the direction of magnetization within the domain. It follows that

$$\langle f_N \rangle = K_m f_N, \quad (3)$$

where  $\langle f_N \rangle$  is the effective nuclear polarization and  $f_N$  is the nuclear polarization which exists within each domain.

## III. SAMPLE FABRICATION AND METHOD OF COOLING

The holmium-indium alloy was prepared by melting the two components in a vacuum furnace in an open tantalum crucible. The indium content was determined to be 7.8% by transmission measurements in the monochromatic neutron beam of a high-resolution crystal spectrometer.<sup>14</sup> Because of the large specific heat of holmium metal below  $1^\circ\text{K}$ , we used a relatively small sample so that the paramagnetic refrigerating salt would be capable of cooling the sample to low temperatures. The alloyed casting was machined to a thickness of 0.0685 cm from which a rectangular slab  $0.762 \times 1.905$  cm was cut. The total weight of the specimen was 0.8744 g, yielding a density of  $8.8 \text{ g cm}^{-3}$ , which is, within error, the same density as pure holmium ( $8.80 \text{ g cm}^{-3}$ ). The sample was sprayed with copper and soldered between two copper sheets with a high-purity tin-lead eutectic solder. The copper sheets were in turn soldered to a bundle of  $\sim 5000$  fine copper wires (No. 40, B & S gauge) which were imbedded in the paramagnetic refrigerating salt (205 g of iron ammonium alum). The salt crystals were grown on the copper wires

<sup>8</sup> W. C. Koehler, J. Appl. Phys. **32**, 20S (1961).

<sup>9</sup> T. A. Kaplan, Phys. Rev. **124**, 329 (1961).

<sup>10</sup> R. J. Elliott, Phys. Rev. **124**, 346 (1961).

<sup>11</sup> W. E. Henry, Phys. Rev. **117**, 89 (1960).

<sup>12</sup> Kei Yosida and Hiroshi Miwa, Suppl. J. Appl. Phys. **32**, 8 (1961).

<sup>13</sup> W. C. Koehler, J. W. Cable, E. O. Wollan, and M. K. Wilkinson, Proceedings of the International Conference on Magnetism and Crystallography, Kyoto, Japan, 1961, Paper 312, Proc. Phys. Soc. Japan (to be published) and (private communication).

<sup>14</sup> V. L. Sailor, H. L. Foote, Jr., H. H. Landon, and R. E. Wood, Rev. Sci. Instr. **27**, 26 (1956).

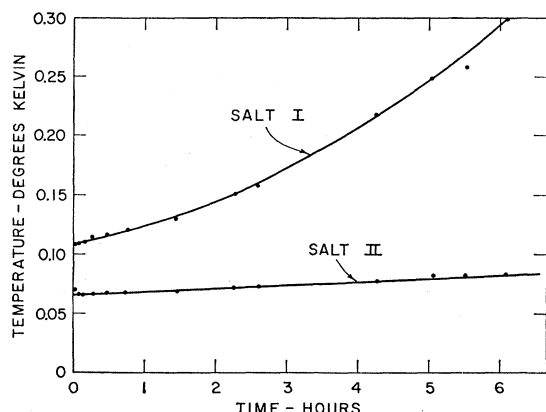


FIG. 1. Typical warm-up curve. The magnetic temperature of the first and second paramagnetic salts are plotted against the time after the adiabatic demagnetization. The heat leaking into salt I comes from the "hot" reservoir which is the 0.95°K liquid helium bath. Salt II warms more slowly since it is shielded by salt I. The nuclear sample came into thermal equilibrium with salt II in less than five minutes.

ensuring a large and intimate copper-salt contact area. To prevent the copper wires from being attacked by the salt, it was necessary to use a varnish-coated wire (e.g., Formvar).

A slightly larger iron ammonium alum salt pill was interposed between the refrigerating salt and the liquid-helium bath. This served as a guard salt which reduced the rate of warmup of the sample. Lead superconducting "heat switches" joined the refrigerating salt to the guard salt and the guard salt to the bath.<sup>15</sup> The liquid helium bath was maintained at a temperature of 0.95°K by pumping. A more complete description of the magnetic refrigerator, the cryostat, and the neutron spectrometer will be given in a forthcoming paper.<sup>16</sup>

The sample was cooled by standard adiabatic demagnetization methods. Heat transport between the salt and the specimen appeared to be very good even at the lower temperatures. The data indicate that the specimen attained thermal equilibrium with the salt in a time too short to measure (less than 5 min). The temperature of the cooling salt and the guard salt were determined by measuring their magnetic susceptibility by the ballistic method. The calibration of susceptibility vs temperature was made at several temperatures between 4.2° and 0.95°K. Magnetic temperatures were converted to thermodynamic temperatures after making corrections for the geometrical shape of the salts.

A typical warmup curve is shown in Fig. 1. After the first few minutes, during which the sample and the

second salt attained thermal equilibrium, the temperature change was very slow, and data could be taken for several hours at essentially a constant temperature. The temperature achieved in the cooling cycle could be varied by adjusting the magnetizing field used in the adiabatic demagnetization. The minimum temperature which could be reached with this particular assembly was about 0.07°K.

#### IV. MEASUREMENT OF THE TRANSMISSION EFFECT

The measurements consisted of determining the transmission of the polarized sample for monochromatic polarized neutrons. The neutrons were polarized alternately parallel and antiparallel to the external magnetic field  $H_0$  which was applied to the sample. Either the holmium or the indium component of the sample could be studied separately by proper choice of the energy of the neutron beam. The holmium data were taken with neutrons having an energy of 3.92 eV, while the indium data were taken at 1.456 eV. These energies correspond respectively to strong neutron resonances in the target nuclei. The effective thickness of the indium was so small that the weak 3.86 eV resonance in indium had negligible effect on the holmium data taken at 3.92 eV.

For slow neutrons ( $s$  wave), a resonance in the cross section corresponds to an excited state of the compound nucleus having a well-defined total angular momentum  $J = I \pm \frac{1}{2}$ , where  $I$  is the spin of the target nucleus. Hence, the transmission of the sample will depend on the  $J$  value of the resonance and on whether the neutrons are polarized parallel or antiparallel to the nuclei. The transmission effect  $\langle \mathcal{E} \rangle$ , which is the measured quantity, is defined by

$$\langle \mathcal{E} \rangle = [(C_P - C_A) / (C_P + C_A)], \quad (4)$$

where  $C_P$  is the counting rate obtained for the transmitted beam when the neutrons are polarized parallel to  $H_0$ , and  $C_A$  the counting rate obtained antiparallel.

If the neutron beam is purely monochromatic and if the beam is not depolarized in passing through the sample, the transmission effect  $\mathcal{E}$  is given by

$$\mathcal{E} = -f_n^0 \tanh(Nt\sigma p) \quad (5)$$

where  $f_n^0$  is the polarization of the neutron beam incident on the target,  $N$  is the density of target nuclei,  $t$  is the sample thickness, and  $\sigma$  is the neutron cross section. The parameter  $p$  is defined as  $p = \rho f_N$ , where  $f_N$  is the nuclear polarization and  $\rho = I / (I + 1)$ ,  $-1$  for  $J = I + \frac{1}{2}$ , or  $I - \frac{1}{2}$ , respectively.<sup>17</sup> More exact equations which take account of beam depolarization, and the efficiency of reversing the neutron polarization, are contained in reference 1. Equation (5) does not apply to most practical cases because of the finite energy resolution of the neutron spectrometer. It can be shown [see reference 1, Eq. (12)] that when spectrometer resolution is considered the transmission effect is given

<sup>17</sup> M. E. Rose, Phys. Rev. **75**, 213 (1949).

<sup>15</sup> For diagram of assembly see Fig. 2 in H. Marshak, H. Postma, V. L. Sailor, F. J. Shore and C. A. Reynolds (to be published).

<sup>16</sup> A complete description of the spectrometer and cryostat will be submitted to Rev. Sci. Instr. in the near future. Brief descriptions were given by H. Marshak, C. A. Reynolds, F. J. Shore, and V. L. Sailor, Bull. Am. Phys. Soc. **3**, 17 (1958); and V. L. Sailor, H. Marshak, F. J. Shore, C. A. Reynolds, and H. Postma, *ibid.* **6**, 275 (1961).

TABLE I. Summary of data taken with 3.92-eV (holmium resonance) neutrons. The observed transmission effect  $\langle \mathcal{E} \rangle$  is listed in column 2. In the third column  $f_n'$  corrects for the fact that the incident neutron beam is not completely polarized and is partially depolarized in passing through the sample (see reference 1). Figure 2 is used to obtain  $p$  from  $\langle \mathcal{E} \rangle / f_n'$ . The net nuclear polarization  $\langle f_N \rangle = p / \rho$ , are fitted to Eq. (8) to obtain the constant  $K_m$  and the argument  $\beta$  of the Brillouin function. The uncertainties listed in column 2 are due to counting statistics only and propagate through the other columns.

$T$ (°K)	$\langle \mathcal{E} \rangle$	$\langle \mathcal{E} \rangle / f_n'$	$p$	$\langle f_N \rangle$
Values are in percent				
4.225	$-1.02 \pm 0.26$	-1.14	3.7	4.8
2.535	$-1.76 \pm 0.33$	-1.96	6.3	8.2
0.95	$-4.32 \pm 0.36$	-4.82	15.8	20.4
0.46	$-6.99 \pm 0.30$	-7.79	25.5	32.8
0.33	$-8.86 \pm 0.30$	-9.88	31.9	41.1
0.07	$-10.47 \pm 0.27$	-11.67	37.0	47.6

by

$$\langle \mathcal{E} \rangle = -f_n' \int_0^\infty R(E' - E) e^{-N\sigma t} \sinh(N\sigma p t) dE' / \int_0^\infty R(E' - E) e^{-N\sigma t} \cosh(N\sigma p t) dE', \quad (6)$$

where  $R(E' - E)$  is the spectrometer resolution function. The quantity  $f_n' = \frac{1}{2}(1 + \phi)(1 - Dt)f_n^0$ , where  $\phi$  is the efficiency for reversing the neutron polarization, and  $1/D$  is the mean free path for neutron spin flip (beam depolarization in the sample). Equation (6) must be evaluated by numerical integration as a function of  $p$  and  $Nt$ . The relationship between  $\langle \mathcal{E} \rangle / f_n'$  and  $p$  is shown in Fig. 2 for the holmium resonance and for a sample thickness,  $Nt = 2.05 \times 10^{21}$  nuclei/cm<sup>2</sup>.

## V. HOLMIUM DATA

### A. Variation of Transmission Effect with Temperature

Table I lists data taken at a neutron energy  $E = 3.92$  eV (the first Ho<sup>165</sup> resonance), at various temperatures. The observed effect  $\langle \mathcal{E} \rangle$  must be divided by  $f_n'$  to account for the fact that the incident beam is not completely polarized and that it is partially depolarized in passing through a sample. The beam polarization  $f_n^0$ , the flipping efficiency  $\phi$ , and the depolarization parameter  $D$  could not be directly measured at the resonance energies because of insufficient beam intensity. However, these quantities were measured in the range 0.07 to 0.3 eV and an extrapolation indicates that  $f_n' \approx 0.90 \pm 0.03$ . The resolution correction is then applied (Fig. 2) to yield  $p$ . In this case it has been established<sup>1</sup> that  $J = I + \frac{1}{2}$ ; hence  $\rho = I / (I + 1) = 7/9$  and  $f_N = (9/7)p$ . The value of the effective nuclear polarization derived from the data by this procedure is designated as  $\langle f_N \rangle$  in Table I.

Within any individual ferromagnetic domain, the nuclear polarization  $f_N$  is given by the Brillouin

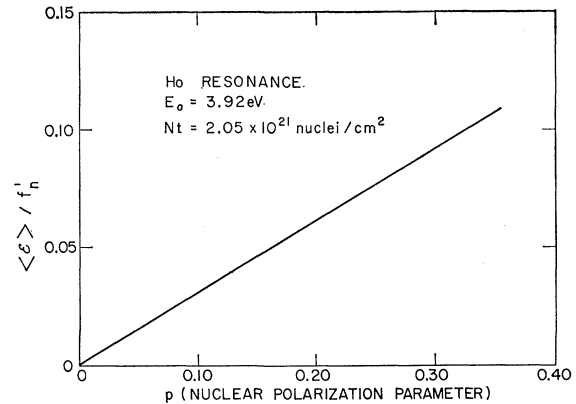


FIG. 2. Calculated transmission effect vs nuclear polarization. The curve shown here was computed from Eq. (6) which takes account of the neutron energy resolution of the spectrometer, the sample thickness  $Nt$ , and the Doppler-broadened Breit-Wigner shape of the resonance.

function,

$$f_N = B_I(\beta) \equiv \frac{2I+1}{2I} \coth\left(\frac{2I+1}{2}\beta\right) - \frac{1}{2I} \coth\left(\frac{\beta}{2}\right), \quad (7)$$

where  $\beta \equiv A/2kT$ ,  $A$  is the hyperfine constant,  $k$  is the Boltzmann constant, and  $T$  is the absolute temperature. Thus, Eq. (3) becomes

$$\langle f_N \rangle = K_m B_I(\beta). \quad (8)$$

The data in Table I were fitted to Eq. (8) to yield the two constants  $K_m$  and  $A/k$ . Because of the form of Eq. (7) it was necessary to resort to a trial-and-error method of fitting.<sup>18</sup> Various methods of weighting the individual points were tested and all calculations yielded essentially the same values. The best fit, shown in Fig. 3, yielded the result,

$$K_m = 0.48 \pm 0.03, \text{ and } A/k = +0.58 \pm 0.03^\circ\text{K}.$$

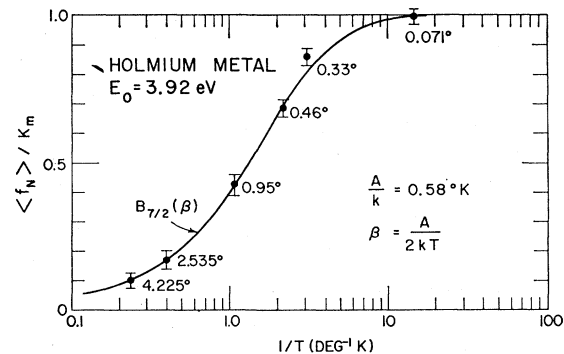


FIG. 3. Observed polarization of holmium nuclei as a function of temperature. The nuclear polarization  $\langle f_N \rangle$  was derived from the experimental data using Fig. 2. The value  $K_m = 0.48$ , and the curve (Brillouin function) which is shown are the best fit of the data to Eq. (8). The argument of the Brillouin function corresponds to a hyperfine interaction constant of  $A/k = 0.58^\circ\text{K}$ .

<sup>18</sup> The procedure of fitting was aided by the table of the Brillouin function, R. I. Schermer, Brookhaven National Laboratory Report BNL 702(T-243), 1961 (unpublished).

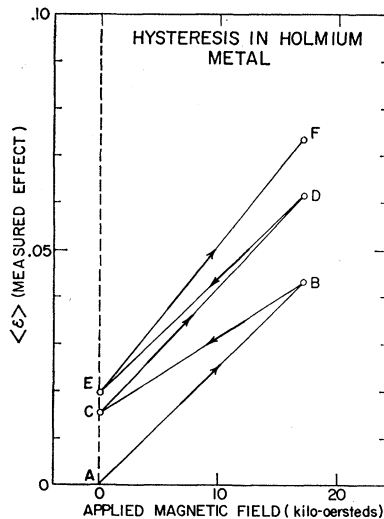


FIG. 4. Hysteresis effects in holmium metal at  $0.1^\circ\text{K}$ . The sample, initially in zero applied field at point A, had not been previously magnetized since being cooled down through the Curie point. The magnetic field was first turned on in going from A to B. The field remained at B for 1.5 h while  $\langle \mathcal{E} \rangle$  was measured. The field was then turned off in going from B to C. The residual effect which is observed at C is due to retentivity. The cycle was repeated from C to D, D to E, and E to F, always turning the field on in the same direction. As is seen from the figure, two cycles are insufficient to reach saturation.

The discrepancy between the  $K_m$  obtained above and the value  $K_m = 0.6$  estimated from the model in Sec. II is unexplained at present. The model is, of course, highly idealized and cannot be viewed too seriously; however, most variations of the model from the simple assumptions we have made would tend to increase the estimated  $K_m$  and thus increase the discrepancy. Probably a more reasonable explanation is that the Ho-In alloy has a different magnetization curve from the specimen of pure Ho used by Henry.<sup>11</sup> Therefore, an effort will be made to measure the magnetization curve for our specimen in the near future.

The value of  $A/k$  is in good agreement with our previous results with the pure metal,<sup>1</sup> and with the specific heat measurements of Gordon *et al.*<sup>3</sup> Our result corresponds to an effective field at the Ho nucleus of  $H_{\text{eff}} = +8.4 \times 10^6$  Oe, the + sign indicating that  $H_{\text{eff}}$  is in the same direction as the external field.

*Note added in proof.*—The quoted value of  $H_{\text{eff}}$  was calculated using the magnetic moment of  $\text{Ho}^{165}$ ,  $\mu = 3.3$  nm, as derived from paramagnetic resonance experiments with holmium ethyl sulfate.<sup>2</sup> With newly calculated values of  $\langle r^{-3} \rangle$  [B. R. Judd and I. Lindgren, *Phys. Rev.* **122**, 1802 (1961)] the nuclear moment is 4.1 nm, which gives  $H_{\text{eff}} = 6.7 \times 10^6$  Oe for the metal. Kondo's value will be reduced to  $7.5 \times 10^6$  Oe. A theoretical estimate of  $H_{\text{eff}}$  due to the contribution of the orbital term alone has been made by Kondo<sup>19</sup> who obtains  $H_{\text{eff}} \approx +9.0 \times 10^6$  Oe. It appears, therefore, that most

<sup>19</sup> J. Kondo, *J. Phys. Soc. Japan* **16**, 1690 (1961).

of the hyperfine interaction which we observe for the holmium nuclei originates from the unpaired  $4f$  electrons.

## B. Magnetic Hysteresis and Retentivity

There are practical difficulties in using our equipment in determining whether or not a particular specimen of holmium alloy is ferromagnetic. However, our data show definitely that the specimen exhibits hysteresis and retentivity. When a holmium specimen is warmed up to room temperature its magnetic history is destroyed. Upon cooling again, the effect  $\langle \mathcal{E} \rangle$  increases each time that the applied magnetic field is recycled between 0 and 17 000 Oe. After four or five such cycles  $\langle \mathcal{E} \rangle$  becomes constant. This behavior, which is attributed to hysteresis, is illustrated in Fig. 4. It will be noted that the effect  $\langle \mathcal{E} \rangle$  does not disappear when the external field is decreased to zero. This can be attributed to the retentivity of the sample.

## VI. INDIUM DATA

A strong resonance in the neutron cross section of  $\text{In}^{115}$  occurs at an energy  $E_0 = 1.456$  eV, which is known to be a  $J = I + \frac{1}{2}$  state from resonance scattering<sup>20</sup> and nuclear polarization measurements.<sup>21,22</sup> We have also verified this assignment using "brute force" polarization of pure In metal.<sup>16</sup> When we observe this resonance with the Ho-In alloy, we find a large transmission effect  $\langle \mathcal{E} \rangle$  which arises from the polarization of the In nuclei (see Table II). Note, however, that the direction of the nuclear polarization is reversed in the alloy from its normal direction in pure indium, i.e., the effective magnetic field  $H_{\text{eff}}$  is opposite to the external field  $H_0$ .

The existence of a negative  $H_{\text{eff}}$  could be attributed to polarization<sup>23</sup> of the core electrons of the indium atom by the surrounding ferromagnetic host material. At present, the exact mechanism for the origin of  $H_{\text{eff}}$  cannot be specified because neither theory nor experiment can distinguish between several interactions which could individually or collectively produce the effect.

TABLE II. Summary of data taken with 1.456-eV (indium resonance) neutrons. A curve similar to Fig. 2 but calculated for the indium cross section and sample content was used to obtain  $p$  from  $\langle \mathcal{E} \rangle / f_N'$ . The value of  $K_m$  obtained from the Ho data, and the values of  $\langle f_N \rangle$  in the last column yielded the argument  $\beta$  of the Brillouin function applying to the indium nuclei.

$T$ ( $^\circ\text{K}$ )	$\langle \mathcal{E} \rangle$	$\langle \mathcal{E} \rangle / f_N'$	$p$	$\langle f_N \rangle$
Values are in percent				
0.95	$+0.26 \pm 0.22$	0.29	-0.31	-0.37
0.205	$+1.17 \pm 0.26$	1.30	-1.59	-1.94
0.123	$+2.19 \pm 0.30$	2.44	-2.99	-3.65
0.071	$+4.00 \pm 0.34$	4.45	-5.45	-6.66

<sup>20</sup> J. A. Moore, *Phys. Rev.* **109**, 417 (1958).

<sup>21</sup> J. W. T. Dabbs, L. D. Roberts, and S. Bernstein, *Phys. Rev.* **98**, 1512 (1955).

<sup>22</sup> A. Stolovy, *Phys. Rev.* **118**, 211 (1960).

<sup>23</sup> R. E. Watson and A. J. Freeman, *Phys. Rev.* **123**, 2027 (1961).

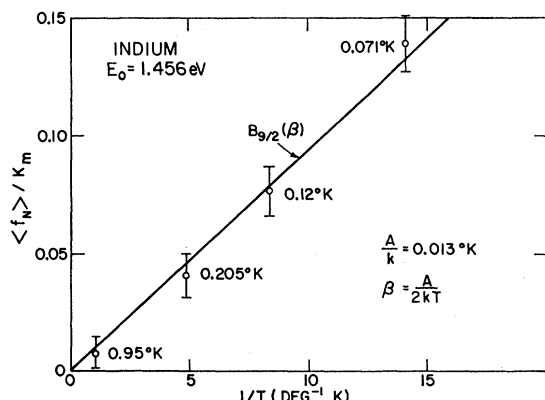


FIG. 5. Observed polarization of indium nuclei as a function of temperature. The value of  $K_m$  obtained from the holmium data was used in this analysis. The curve shown is the Brillouin function which gave the best fit, corresponding to a hyperfine interaction constant  $A/k = -0.013^\circ\text{K}$ . The sign of  $A/k$  is determined by the direction of the observed effect  $\langle \mathcal{E} \rangle$ , and the known value of  $J$  for the 1.456-eV indium resonance.

The data listed in Table II and plotted in Fig. 5 can be fitted to Eq. (8) in a manner similar to that used for fitting the Ho data. Unfortunately, the indium data lie on the linear portion of the Brillouin function and thus an independent solution for  $K_m$  is excluded. We have, therefore, assumed that the value  $K_m = 0.48$ , obtained from the holmium data, is also valid for the indium component. With this assumption, the hyperfine splitting constant for the indium is  $A/k = -0.013 \pm 0.002^\circ\text{K}$  which corresponds to an effective field at the indium nucleus of  $H_{\text{eff}} = -130\,000$  Oe. While the

sign of  $H_{\text{eff}}$  is certainly negative, the magnitude must be regarded as provisional because of the uncertainty in  $K_m$  for the indium component. Before the hyperfine phenomenon can be quantitatively interpreted, more work on Ho-In alloys will be necessary including studies of the phase diagrams and the crystal structures.<sup>24</sup>

The linearity of  $\langle \mathcal{E} \rangle$  vs  $T^{-1}$  (Fig. 5) demonstrates that this sample is in thermal equilibrium with the refrigerating salt. If there were a large heat input into the sample due to eddy current heating, vibration, etc., the linearity would be destroyed.

#### ACKNOWLEDGMENTS

The authors gratefully acknowledge the able and patient assistance of E. Caruso, J. P. Roberge, R. D. Schmidt, R. Smith, and J. P. Smolski.

<sup>24</sup> The phases and crystal structure of the holmium-indium system have not been studied; however, dysprosium-indium forms the intermetallic compound  $\text{Dy}_2\text{In}$  (tetragonal) for small indium content, followed by  $\text{DyIn}$ , etc., as the indium content is increased [see N. C. Baenziger and J. L. Moriarty, Jr., *Acta Cryst.* 14, 948 (1961)]. It is reasonable that the holmium-indium system will form similar phases, in which case our specimen was probably actually composed of regions of  $\text{Ho}_3\text{In}$  dispersed in pure Ho. For such structure the value of  $K_m$  could be appreciably different for the holmium and indium components since only  $\sim 25\%$  of the Ho but all of the In atoms would be involved in the intermetallic compound. On the other hand, if  $\text{Ho}_3\text{In}$  is tetragonal (as in  $\text{Dy}_2\text{In}$ ) it would exhibit strong magnetic anisotropy which would yield  $K_m$  similar in magnitude to that which we have calculated in Sec. II for pure Ho. A further possibility must be considered, namely that part of the indium was present in the specimen in the form of inclusions of pure indium. One casting which was prepared gave evidence of such inclusions, although the specimen used in the experiments did not appear to suffer from inhomogeneities of this type.